Journal of Sustainability Science and Management
Volume 15 *Number* 3, April 2020: 3-9

eISSN: 2672-7226

THE INFLUENCES OF Cr_2O_3 ADDITION ON STRUCTURAL PROPERTIES OF $NdBa_2Cu_3O_{7-\delta}$ SUPERCONDUCTOR

AIMA RAMLI*[1,2], NADIA MANHORIL[3] AND WAN NURDIYANA WAN MANSOR[3]

[1]*Advanced Nano Materials (ANoMA) Research Group, Faculty of Science and Marine Environment,* [2]*Ionic State Analysis (ISA) Laboratory, Faculty of Science and Marine Environment,* [3]*Faculty of Ocean Engineering Technology and Informatics, Universiti Malaysia Terengganu, Terengganu, 21030 Kuala Nerus, Malaysia.*

**Corresponding author: aima.ramli@umt.edu.my*

Abstract: $NdBa_2Cu_3O_{7-\delta}$ (NdBCO) superconductor is one of high temperature superconductors with high upper critical field that has the ability to conduct electric current without resistance and without losing any energy when cooled below a certain critical temperature (T_c). NdBCO bulk materials are known to have superior superconducting properties than $YBa_2Cu_3O_{7-\delta}$ (YBCO) and can be added with any suitable element to enhance and sustain their superconducting properties. In this research, Cr_2O_3 nanoparticles were added in NdBCO superconductor with different weight percentages which are 0.0, 0.3, 0.6, and 0.9 wt% and the influences of the addition of Cr_2O_3 nanoparticles in NdBCO were investigated. The samples of NdBCO added with Cr_2O_3 nanoparticles were synthesized by solid state reaction method. Solid state reaction method was chosen due to reduced pollution, time savings and homogeneous reactions. Then, samples were characterized by Thermogravimetric Analysis (TGA), X-Ray Diffraction (XRD) and Scanning Electron Microscope (SEM). The optimum temperature for sintering that was determined by TGA is in the range of 900 °C to 920 °C. The orthorhombic phase is shown in all samples with dominantly Nd-123 and Cr_2O_3 depicted from X-ray diffraction analysis. SEM analysis revealed that the microstructure of samples has the largest average grain size at 0.3 wt% of Cr_2O_3 concentration compared with other samples due to the high value in orthorhombicity which is related to the oxygen content. The oxygen deficiency plays a crucial role for affecting high temperature superconductivity.

Keywords: $NdBa_2Cu_3O_{7-\delta}$, superconductor, sustain, solid state method, nanoparticles.

Introduction

There is some resistance to the motion of electrons through the material whenever electrical current flows for most materials, which are normal conductors. To replace the energy dissipated by the resistance, it is necessary to apply a voltage to keep the current going. Electronic is based on components in which the resistance changes under control of an input voltage as these components are made of semiconductors. A superconductor is a material with no resistance at all. According to Sheahen (1999), the first metal found to be a superconductor was mercury, soon after the invention in 1908 of a cryogenic refrigerator that could attain the temperature at which helium becomes a liquid at 4.2 K (452°F). In the subsequent 60 years, more superconductors were found at these low temperatures. By the 1960s, certain alloys of niobium were made that become superconductors at 1023 K (Cernusko *et al*., 1977).

The discovery of superconductivity at around 90 K in $YBa_2Cu_3O_{7-\delta}$ (YBCO) has opened up new horizons in the field of superconductivity. This is followed by the discovery of other high temperature superconductors (HTSC) such as the bismuth, thallium and mercury systems with transition temperatures above the boiling point of liquid nitrogen (Kazakof *et al*., 1997; Sheng & Herman, 1988). Until 1988, all the known superconductors were *p*-type, which led many to postulate that there would never be an *n*-type copper oxide superconductor. Up to date, the first and so far, the only *n*-type superconductor was discovered by Takagi *et al.* (1989) from the University Of Tokyo. The new superconductor

was based on neodymium copper oxide (Nd_2CuO_4). The structure of Nd_2CuO_4 is similar to La_2CuO_4 whereas lanthanum prefers nine oxygen neighbours. The smaller neodymium ion is usually coordinated to eight oxygen atoms. In the Nd_2CuO_4 compound the oxygen atoms form a square prism around the neodymium atoms. As a result, the copper atoms are coordinated to four oxygen atoms in a square planar geometry. In the superconductors based on Nd_2CuO_4, some of the neodymium atoms are replaced by cerium or thorium, forming a solid solution. Both cerium and thorium are valence 4+ and are of an appropriate size to substitute for some of the neodymium of valence 3+. Hence, they can form the solid solutions $Nd_{2-x}Ce_xCuO_4$ and $Nd_{2-x}Th_xCuO_4$. When x equals 0.17, these materials reach their highest transition temperatures, near 25 K. These materials remain the subject of active research because they have subtle chemical features that are not yet understood and that are relevant to the nature of the charge carriers (Robert, 1990).

From the materials processing point of view $NdBa_2Cu_3O_{7-\delta}$ (NdBCO) has been of great interest because it has a wider solidification range and exhibits a much higher peritectic decomposition temperature than the widely studied $YBa_2Cu_3O_{7-\delta}$ (YBCO). The structure and the superconducting properties of NdBCO with various oxygen contents have also been reported. High transition temperature up to 95 K and sharp transition when prepared by melt processing in air was also shown by NdBCO (Abd-Shukor *et al.*, 2001).

Ramli *et al*. (2016 & 2018) proved that as the addition of magnetic nanoparticles, Nd_2O_3, Sm_2O_3 and Gd_2O_3 increased, the average grain sizes decreased showing that the poor grain connectivity was due to porosities and weak links. The volume fractions of non-superconducting phase, Y-211 rapidly increased in all systems, thus affecting the T_c and J_c in the Y123 system and it might be due to the local differences in the size of Y-211.

In this work, in order to investigate the influences of Cr_2O_3 magnetic nanoparticles with x = 0.0, 0.3, 0.6 and 0.9 wt% on structural properties, $NdBa_2Cu_3O_{7-\delta}$ superconductos have been synthesized via solid state reaction method.

Materials and Methods

Materials Preparation

All samples were prepared via solid state reaction route by mixing stoichiometric amount of highly pure Nd_2O_3 (Alfa Aesar, 99.9%), $BaCO_3$ (Alfa Aesar, 99.8 %), and CuO (Alfa Aesar, 99.7 %) at ratio 1:2:3 as shown in Equation 1.

$$Nd_2O_3 + 4BaCO_3 + 6CuO + ½O_2 \rightarrow 2NdBa_2Cu_3O_{7-\delta} + 4CO_2 \quad [1]$$

The powders were ground for one hour using agate mortar and pestle. The mixture was transferred into a crucible boat before being calcined using furnace at 900 °C at heating rate of 2 °C/min for 12 hours and followed by cooling in air. Next, intermediate grinding for one hour was needed before samples were heated again. Then, Cr_2O_3 (Aldrich, 99.9%) nanoparticles (x = 0.0, 0.3, 0.6, and 0.9 wt%) was added into $NdBa_2Cu_3O_{7-\delta}$ samples respectively and ground to form homogenous powder mixture and pressed into pellets of 13 mm diameter and 5 mm thickness using Specac automatic hydraulic press and sintered using furnace at 920 °C at heating rate of 2 °C/min for 12 hours.

Materials Characterization

Thermogravimetry Analysis (TGA)

The thermal properties of the precursor powder were analysed by Mettler Toledo TGA/SDTA 851 from 30 ºC to 900 ºC at a heating rate of 10 ºC/min. Samples of 2g were approximately placed in aluminium pans under a dynamic flow of nitrogen 50mL/min.

X-Ray Diffraction (XRD)

The phase composition of samples was performed by using a Rigaku Mini Flex II Desktop X-ray diffractometer with Cu-K_α. The mixture of finely ground and homogenized $NdBa_2Cu_3O_{7-\delta}$ with different doping compositions were analysed with XRD. The powder was placed on a glass

holder and placed at the sample stage. The scanning was carried out from 20° to 80° at a step width of 0.02°.

Scanning Electron Microscope (SEM)

SEM measurement was performed by using JEOL JSM-6360LA. This process required extra steps and pellets were carefully fractured inti small pieces using a pestle and mortar. To get better imaging, the surface and fractured (cross section) pellets were then coated with gold before analysing the samples.

Results and Discussion

Thermogravimetry Analysis (TGA)

Figure 1 shows the thermogravimetric analysis (TGA) result. TGA measured the weight loss and it represents the thermal decomposition behaviour of $NdBa_2Cu_3O_{7-\delta}$. The weight loss indicated the dehydration of moisture and water from the lattice of copper oxide occurring at temperature below 250 °C. At range 250 °C to 375 °C, the weight losses were due to the decomposition of neodymium oxide. Barium carbonate decomposes into barium oxide at temperature 375 °C to 800 °C. At 900 °C, Nd-123 phase is shown. Nd-123 phase indicates the stoichiometric quantities constituting elements of Nd:1 Ba:2 Cu:3 (Fujihara et al., 1999). From this graph, it can be concluded that at temperature above 950 °C above, Nd-123 phase started to destroy. This is due to oxygen loss and the melting of the superconductor. Based on this TGA curve result, the temperatures that range from 900 °C to 920 °C are suggested as optimum sintering temperature for $NdBa_2Cu_3O_{7-\delta}$.

X-ray Diffraction (XRD)

The X-ray diffraction (XRD) analysis is depicted in Figure 2. It was found that all samples show the orthorhombic structure with Nd-123 phase and impurities of Cr_2O_3 nanoparticles. There is only one significant peak for Cr_2O_3 from the graph. The intensity peak increased as the concentration of Cr_2O_3 increased. From the XRD analysis, lattice parameters of the samples can be obtained as presented in Table 1.

It is noticed that the lattice constants *a*, *b* and *c* slightly change with the different concentration of nano-Cr_2O_3 which indicated that nano-Cr_2O_3 cations were well incorporated into the $NdBa_2Cu_3O_{7-\delta}$ crystal. The difference between *a* and *b* parameters reduced the orthorhombicity. The high value of orthorhombicity of $NdBa_2Cu_3O_{7-\delta}$ samples indicated high oxygen content and that consequently could give better superconducting properties (Jin Fei *et al*., 2017). Figure 4.3 shows the orthorhombic value of $NdBa_2Cu_3O_{7-\delta}$ with various concentrations of Cr_2O_3 doped to it. The orthorhombicity decreased as the concentration of Cr_2O_3 nanoparticles increased. This may be attributed to the oxygen deficiency which might affect the superconducting properties.

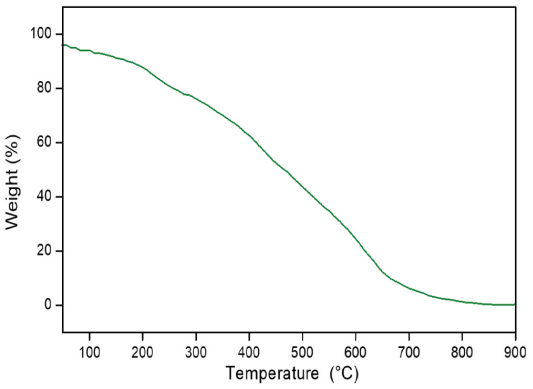

Figure 1: Thermogravimetric analysis of $NdBa_2Cu_3O_{7-\delta}$ powder

Table 1: Lattice parameters, *a*, *b* and *c* axes for $NdBa_2Cu_3O_{7-\delta}$ superconductor doped with various Cr_2O_3 concentrations

NdBCO + *x* wt% of Cr_2O_3	***a*** **(Å)**	***b*** **(Å)**	***c*** **(Å)**	**V (Å^3)**	**δ = [(b – a)/(b +a)]**
x = 0.0	3.8641	3.9189	11.7640	178.1430	0.0070
x = 0.3	3.8649	3.9243	11.7830	178.7130	0.0076
x = 0.6	3.8732	3.9149	11.7397	178.0110	0.0054
x = 0.9	3.8779	3.9161	11.7645	178.7510	0.0046

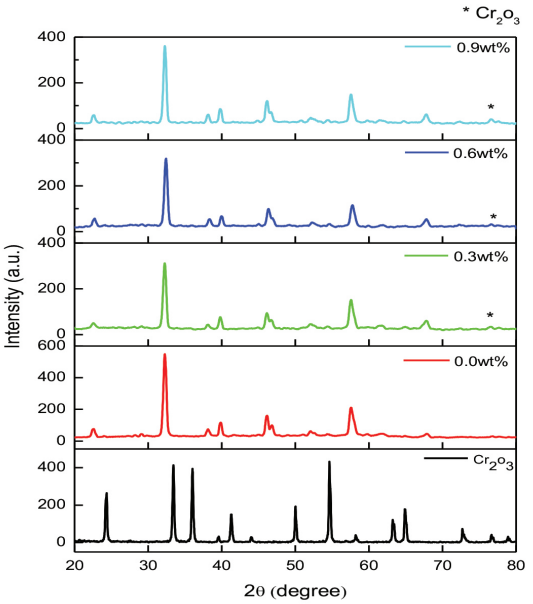

Figure 2: XRD patterns of Cr_2O_3 and $NdBa_2Cu_3O_{7-\delta}$ samples doped with various Cr_2O_3 concentrations

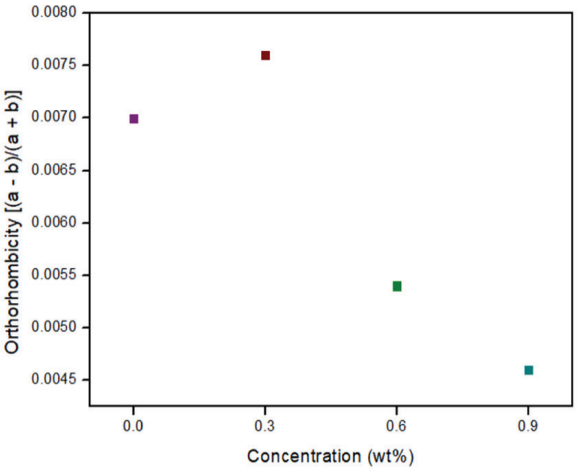

Figure 3: Calculated orthorhombicity versus $NdBa_2Cu_3O_{7-\delta}$ doped with various concentrations of Cr_2O_3

Scanning Electron Microscope (SEM)

SEM images of pure $NdBa_2Cu_3O_{7-\delta}$ and $NdBa_2Cu_3O_{7-\delta}$ with addition of 0.3, 0.6 and 0.9 wt% of Cr_2O_3, for surface morphology and cross section (fractured) morphology are shown in Figure 4 and Figure 5 respectively. The average size of grains for the samples was determined from 100 grains randomly measured using Image-J software. From these figures, what is clear is that as the concentration of Cr_2O_3 increased, the average grain size of the samples also increased. However, the average grain size for $NdBa_2Cu_3O_{7-\delta}$ doped with 0.6 wt% of Cr_2O_3 is the smallest at 2.02 µm compared with pure $NdBa_2Cu_3O_{7-\delta}$, $NdBa_2Cu_3O_{7-\delta}$ adding with 0.3 wt% and 0.9 wt% of Cr_2O_3 which are 3.81 µm, 6.83 µm and 4.76 µm, respectively for surface morphology.

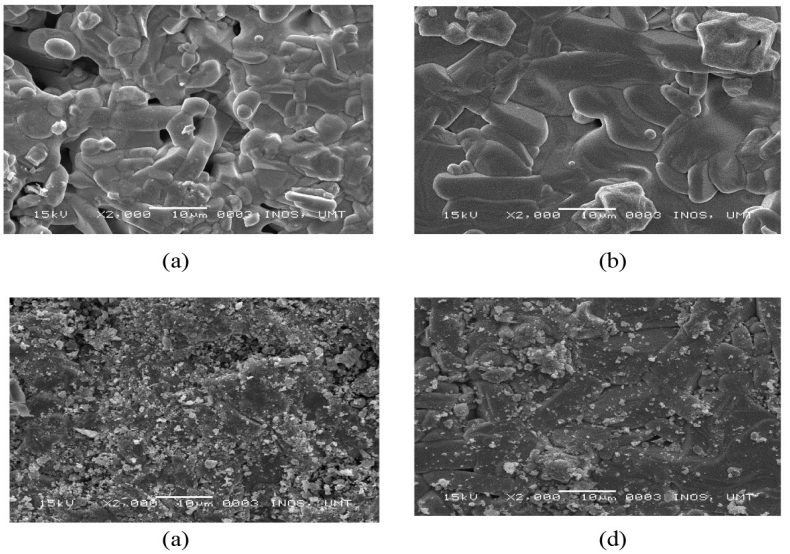

Figure 4: SEM micrographs of the surface of $NdBa_2Cu_3O_{7-\delta}$ doped with (a) 0.0 wt%, (b) 0.3 wt%, (c) 0.6 wt% and (d) 0.9 wt% of Cr_2O_3

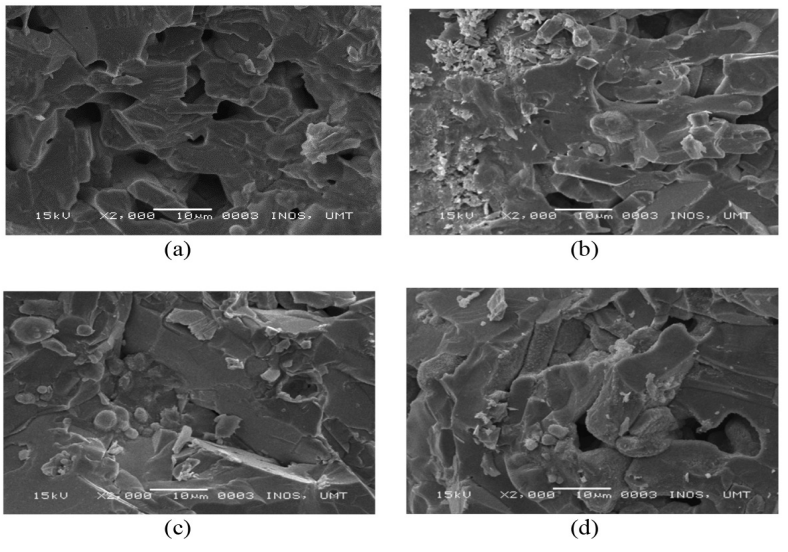

Figure 5: SEM micrographs of the cross section (fractured) of $NdBa_2Cu_3O_{7-\delta}$ doped with (a) 0.0 wt%, (b) 0.3 wt%, (c) 0.6 wt% and (d) 0.9 wt% of Cr_2O_3

The variation of grain size also indicates that Cr_2O_3 nanoparticles were well incorporated in $NdBa_2Cu_3O_{7-\delta}$ samples. The average grain size is the highest at Cr_2O_3 concentration of 0.3 wt% and the smallest at 0.6 wt% compared to other concentration. The reduction of grain size indicates to poor connectivity with low angle between grains. Furthermore, the samples with small grain size and big grain boundaries might contribute to low critical temperature value which allow the supercurrent to flow across barrier with high difficulty (Topal & Eyyuphan, 2010). In addition, the grain size is also effected from the inhomogeneity of the samples during samples preparation.

Conclusion

The $NdBa_2Cu_3O_{7-\delta}$ bulk samples doped with nano-Cr_2O_3 (x = 0.0, 0.3, 06 and 0.9 wt%) were successfully synthesized by solid state reaction method. The XRD analysis found that all samples show orthorhombic structure with Nd-123 phase and impurities of Cr_2O_3 nanoparticles. However, the orthorhombicity decreased as the concentration of Cr_2O_3 increased due to the oxygen deficiency. Besides, it is revealed from SEM that the grain size of the $NdBa_2Cu_3O_{7-\delta}$ doped with 0.6 wt% of Cr_2O_3 samples is smaller compared with pure $NdBa_2Cu_3O_{7-\delta}$, $NdBa_2Cu_3O_{7-\delta}$ doped with 0.3 wt% and 0.9 wt% of Cr_2O_3. The optimum concentration for Cr_2O_3 nanoparticles doping is at 0.3 wt% as it has the highest orthorhombicity which resulted from high oxygen content.

Acknowledgements

The authors would like to thank the supports to Advanced Nano Materials (ANoMa) Research Group and the Ionic State Analysis (ISA) Laboratory of the Faculty of Science and Marine Environment and the Faculty of Ocean Engineering Technology and Informatics, Universiti Malaysia Terengganu for the valuable support given.

References

Abd-Shukor, R., Abdullah, I., & Hamadneh, I. (2001). Electrical properties and longitudinal modulus of superconductor/polymer $NdBa_2Cu_3O_{7-\delta}$ /PVC composites. *Journal of Materials Science,* 36, 853-857.

Al-Saadi, T. M. & Hameed, N. A. (2015). Synthesis and structural characterization of Cr_2O_3 nanoparticles prepared by using $Cr(NO_3)_3.9H_2O$ and triethanolamine under microwave irradiation. *Advances in Physics Theories and Applications, 44*, 139-144.

Cernusko, V., Jergel, M., & Cabelka, D. (1977). Continuous Nb_3Ge superconducting tape prepared by chemical vapour deposition. *Solid State Communications*, *23*, 487-488.

Elesin, V. F. (2007). Meissner effect in superconductors with a finite pair momentum. *Journal of Experimental and Theoretical Physics*, *104*(5), 819-821.

Essen, H. (2012). Meissner effect, diagmagnetism, and classical physics – a review. *American Journal of Physic, 80*(2), 164.

Fujihara, S., Murakami, G., Kimura, T., & Masuda, Y. (1999). Interfacial reaction between Ag and $NdBa_2Cu_3O_{7-\delta}$. *Journal of the European Ceramic Society*, *19*, 1551-1554.

Gombos, M., Varesi, E., Tedesco, P., Vecchione, A., & Pace, S. (2008). A simple statistical phenomenological model for cation substitutions in $Nd_{(1+x)}Ba_{(2-x)}Cu_{(3)}O_{(7)-(\delta+x/2)}$. *Philosophical Magazine*, *88*, 1389-1399.

Hakuraku, Y., Mori, Z., Koba, S., Yokoyama, N., Doi, T., & Inoue, T. (1999). Critical parameters in the sputter-deposition of $NdBa_2Cu_3O_{7-\delta}$ thin films. *Superconductor Science and Technology, 12*, 481.

Kazakov, S. M., Chailout, C., Bordet, P., Capponi, J. J., Nunez-Reguiro, M., Rysak, A., Tholence, P., Radaell, G., Putilin, S. N., & Antipov, E. V. (1997). Discovery of a second family of bismuth-oxide-based superconductors. *Nature*, *390*, 148-150.

Koblischka, M. R., Dalen, A. J. J., Higuchi, T., Yoo, S. I., & Murakami, M. (1997). Analysis of pinning in $NdBa_2Cu_3O_{7-\delta}$ superconductors. *Physical Review B, 58*(5), 2863.

Makhlouf, S. A., Zinab, H. B., Al-Attar, H., & Moustafa, M. S. (2013). Structural, morphological and electrical properties of Cr_2O_3 nanoparticles. *Material Sciences and Engineering B*, *178*(6), 337-343.

Malashevich, A., Coh, S., Souza, I., & Vanderbilt, D. (2012). Full magnetoelectric response of Cr2O3 from first principles. *Physical Review B*, *86*, 1-3.

Malozemoff, A. P., Mannhart, J., & Scalapino, D. (2005). High-temperature superconductors get to work. *Physics Today*, *4*, 41-47.

Mollah, S., Biswas, B., Haldar, S., & Ghosh A. J. (2017). Carrier concentration induced transformations and existence of pseudogap in $NdBa_2Cu_3O_{7-\delta}$. *Physica C: Superconductivity and Its Application*, *539*, 40-43.

Ramli, A. (2015). *Structural and electrical properties of YBCO added with Nd_2O_3, Gd_2O_3 and Sm_2O_3 nanoparticles* (doctoral dissertation). University Putra Malaysia, Serdang.

Robert, J. C. (1990). Superconductors beyond 1-2-3. *Scientific America*, *263*(2), 42-49.

Rong, T., Wang, K., Ting, W., Yang, M., Qizhong, L., Zhang, S., Liangmeng, Z., Takashi, G., Shi, J., & Hitoshi, O. (2018). Structural study of epitaxial $NdBa_2Cu_3O_{7-x}$ films by laser chemical vapor deposition. *RSC Advance*, *8*, 19811.

Salama, A. H., El-Hofy, M., Rammah, Y. S. & Elkhatib, M. (2016). The influence of magnetic nano metal oxides doping on structure and electrical properties of YBCO superconductor. *Advance in Natural Sciences: Nanoscience and Nanotechnology, 7*(1), 1-8.

Schoofs, B., Mouganie, T., Glowacki, B. A., Cloet, V., Hoste, S., & Driessche, I.V. (2006).Synthesis of highly textured superconducting $NdBa_2Cu_3O_{7-y}$ thin films using an aqueous inorganic sol-gel dip coating technique. *Journal of Physics: Conference Series, 43*, 187.

Sheahen, T. P. (1999). Introduction to High-Temperature Superconductivity. *Selected Topics in Superconductivity*, *10*, 1-19.

Sheng, Z. Z. & Herman, A. M. Bulk superconductivity at 120 K in the Tl-Ca/Ba-Cu-O system. *Nature*, *332*, 138-139.

Smits, F. M., (1957). Measurements of Sheet Resistivity with the Four Point Probe. *The Bell System Technical Journal*, *37*, 371.

Takagi, H., Tokura, Y., & Uchida, S. (1989). Similarity and dissimilarity in transport properties of electron and hole doped high T_c cuprates. *Physica C: Superconductivity and Its Application*, *162*, 1001-1002.

Topal, U. & Eyyuphan Yakinchi, M. (2010). Effects of grain boundaries on electrical and magnetic properties of melt-processed $SmBa_2Cu_3O_x$ superconductors. Material Chemistry and Physics, *119*, 182-187.